STATISTICS, OPTIMIZATION AND INFORMATION COMPUTING
Stat., Optim. Inf. Comput., Vol. **12**, Month 2024, pp 0–19.
Published online in International Academic Press (www.IAPress.org)

Julia sets of transcendental functions via a viscosity approximation-type iterative method with s-convexity

Iqbal Ahmad [1,*], Mohammed Sajid [1], Rais Ahmad [2]

[1]*Department of Mechanical Engineering, College of Engineering, Qassim University, Saudi Arabia*
[2]*Department of Mathematics, Aligarh Muslim University, Aligarh 202002, India*

Abstract In this article, we explore and analyze the different variants of Julia set patterns for the complex exponential function $W(z) = \alpha e^{z^n} + \beta z^2 + \log \gamma^t$ and complex sine function $T(z) = \sin(z^n) + \beta z^2 + \log \gamma^t$, where $n \geq 2, \alpha, \beta \in \mathbb{C}, \gamma \in \mathbb{C}\backslash 0$, and $t \in \mathbb{R},\ t \geq 1$ by employing a viscosity approximation-type iterative method with s-convexity. We utilize a viscosity approximation-type iterative method with s-convexity to derive an escape criterion for visualizing Julia sets. This is achieved by generalizing the existing algorithms, which led to visualization of beautiful fractals as Julia sets. Additionally, we present graphical illustrations of Julia sets to demonstrate their dependence on the iteration parameters. Our study concludes with an analysis of variations in the images and the influence of parameters on the color and appearance of the fractal patterns. Finally, we observe intriguing behaviors of Julia sets with fixed input parameters and varying values of n.

Keywords Algorithms, Escape criteria, Julia sets, Fractals, Iterative methods, Convexity

AMS 2010 subject classifications 70K55, 28A10, 39B12, 47H10

DOI: 10.19139/soic-2310-5070-1918

1. Introduction

The fascinating field of fractal mathematics has attracted the interest of scientists, mathematicians, and artists, offering profound insights into the intricate balance of complexity and order within the natural world. Among the vast array of mathematical shapes and patterns, Julia sets have emerged as a focal point of study, displaying mesmerizing visual representations and intriguing mathematical relationships. Named after the French mathematician Gaston Julia, these sets lie at the core of the broader field of complex dynamics, constructed through iterations of complex functions that concentrate on specific values within the complex plane. The work of another prominent mathematician, P. Fatou [7], has extended the study of Julia sets by introducing the Fatou set as their complement within the domain, see e.g., [1, 4, 5, 6, 13, 14, 15, 16, 17].

One of the most fascinating aspects of Julia sets is their complex nature. The term "fractal" derived from the Latin language, meaning "split" or "break", accurately describes these self-similar patterns in complex graphics. Fractals, with their infinitely complex and similar patterns, find numerous real-life applications and are prevalent in nature, effectively describing phenomena such as leaf patterns, tree branches, lightning, clouds, rivers, and crystals. The importance of fractals extends to various fields, playing a vital role in surveying or investigating various natural or living structures, including microbial culture. Additionally, fractal theory is widely employed in cryptography, image compression, encryption, radar systems, computational architectural design, and engineering models, which underscores its wide and influential applications in [13].

*Correspondence to: Iqbal Ahmad (Email: i.ahmad@qu.edu.sa). Department of Mechanical Engineering, College of Engineering, Qassim University, Saudi Arabia.

ISSN 2310-5070 (online) ISSN 2311-004X (print)

In the existing literature, numerous studies have explored the application of explicit and implicit iteration schemes in constructing fractal sets. In [2], Ashish et al. utilized Noor iteration to construct Julia sets. Subsequently, Cho et al. [3] expanded upon the results of Ashish et al. by employing s-convex combination. Kumari et al. demonstrated the fractal patterns obtained through the iterative method introduced by Abbas and Nazir in [9]. Recent studies include the utilization of Picard-Mann iteration with s-convexity [18] and Picard-Mann iteration [21] for constructing Julia sets.

Moreover, a generalization of the Halpern iteration, a viscosity-type iteration, was introduced in [8] for constructing Julia sets and biomorphs. Within the implicit group of iteration schemes applied in constructing Julia sets, examples include the Jungk-Noor iteration [22], the DK-iterative scheme and S-iteration with h-convexity [23, 24], the Jungk-CR iteration and Jungk-CR iteration with s-convexity [10, 20], the Jungk-P iteration with s-convexity [9], and the Jungk–S iteration with s-convexity [11]. Notably, iteration schemes extend beyond Mandelbrot and Julia sets, finding applications in the generation of various fractal types such as biomorphs [6, 8, 10], inversion fractals [4], and root-finding fractals [4, 6].

In the majority of studies focusing on the Julia set, researchers commonly employ the n^{th} degree polynomial in the form of $z^n + c$. However, in a distinctive approach, Tanveer et al. [19, 21] introduced a modification to the constant term in this function and a new fixed point iteration. Instead of c, they proposed using $\log(c^t)$, where $t \in \mathbb{R}$ and $t \geq 1$. Moreover, they chose to utilize the Mann and Picard-Mann iterations and furnished a proof for the escape criterion applied in the escape-time algorithm that generated the Mandelbrot sets images in their study.

Motivated by the incorporation of the logarithmic function for the constant term c, our paper adopts a similar approach by replacing the constant c with $\log(c^t)$, where $t \in \mathbb{R}$ and $t \geq 1$. Furthermore, instead of the Mann and Picard-Mann iterations, we employ the viscosity approximation-type iterative method with s-convexity, rigorously establishing escape criteria for the considered iterations. Our study encompasses the presentation and analysis of graphical examples. Inspired by Tanveer et al. [21], the present work investigates Julia sets of complex exponential function $W(z) = \alpha e^{z^n} + \beta z^2 + \log \gamma^t$ and complex sine function $T(z) = \sin(z^n) + \beta z^2 + \log \gamma^t$, where $n \geq 2, \alpha, \beta \in \mathbb{C}, \gamma \in \mathbb{C}\backslash 0$, and $t \in \mathbb{R},\ t \geq 1$, utilizing a viscosity approximation-type iterative method with s-convexity to develop the escape criterion.

The remainder of the paper is structured as follows: In Section 2, we provide fundamental definitions and results essential for accomplishing the objectives of this paper. Section 3 is dedicated to the investigation of escape criteria for the viscosity approximation-type iterative method with s-convexity, focusing on both the complex exponential function $W(z) = \alpha e^{z^n} + \beta z^2 + \log \gamma^t$ and complex sine function $T(z) = \sin(z^n) + \beta z^2 + \log \gamma^t$. In Section 4, we present some graphical examples of Julia sets obtained using the proposed approach. These examples demonstrate the correlation between the size, color, and appearance of the fractal patterns of the generated Julia sets and the values of the parameters. Finally, in Section 5, we conclude our work.

2. Preliminaries

Definition 2.1 (Julia set [7])
Let $p : \mathbb{C} \to \mathbb{C}$. The filled Julia set of p is denote by J_p and is defined as

$$J_p = \{z \in \mathbb{C} : \{|p^k(z)|\}_{k=0}^{\infty} \text{ is bounded}\}.$$

where p^k denotes the k times composition of the function p. Noticeably, it is a set of complex numbers for which the orbits do not converge to a point at infinity. The Julia set of p is the boundary of J_p, that is, $J_p = \partial J_p$.

Definition 2.2 (s-convex combination [15])
Let $z_1, z_2, z_3, \cdots, z_n \in \mathbb{C}$ and $s \in (0, 1]$. The s-convex combination is described as

$$\lambda_1^s z_1 + \lambda_2^s z_2 + \lambda_3^s z_3 + \cdots + \lambda_n^s z_n.$$

where $\lambda_k \geq 0$ and $\sum_{k=1}^{n} \lambda_k = 1$, for $k \in \{1, 2, 3, \cdots, n\}$.

For $s = 1$, the s-convex combination diminishes to the standard convex combination.

Let us consider the following complex mappings $W, T, p : \mathbb{C} \to \mathbb{C}$ as:

$$W(z) = \alpha e^{z^n} + \beta z^2 + \log \gamma^t$$
$$T(z) = \sin(z^n) + \beta z^2 + \log \gamma^t.$$

where $n \geq 2, \alpha, \beta \in \mathbb{C}, \gamma \in \mathbb{C}\backslash\{0\}$ and $t \in \mathbb{R},\ t \geq 1$. Moreover, let $p(z) = az + b$ be a complex contraction mapping with $a, b \in \mathbb{C}$ and $|a| < 1$.
In the manuscript, let $\eta = \frac{\log(\gamma^t)}{\gamma}$. Consequently, we can express $\log(\gamma^t) = \eta\gamma$.
Let $p, W, T : \mathbb{C} \to \mathbb{C}$ be complex-valued mappings such that p is a contraction mapping. In the complex plane, consider the sequence $\{z_k\}_{k=0}^{\infty}$ of iterates for any starting point $z_0 \in \mathbb{C}$, with parameters $\mu, \nu \in (0, 1)$, and $k \geq 0$, is referred to as the viscosity approximation-type iterative method with s-convexity, and it is expressed as:

$$\begin{cases} z_{k+1} = \mu^s p(z_k) + (1-\mu)^s y_k, \\ y_k = \nu^s z_k + (1-\nu)^s W(z_k), \end{cases} \tag{2.1}$$

and

$$\begin{cases} z_{k+1} = \mu^s p(z_k) + (1-\mu)^s y_k, \\ y_k = \nu^s z_k + (1-\nu)^s T(z_k). \end{cases} \tag{2.2}$$

Remark 2.1
The viscosity approximation-type iterative method with s-convexity reduces to:

- The viscosity approximation-type iterative method [21] when $s = 1$.
- The Halpern iteration [8] when $p(z) = b$ and $s = 1$.
- The viscosity approximation method [12] when $\nu = 0$ and $s = 1$.

To generate fractals and escape limitations are the basic key to run the algorithms. Since it is well known that $|\sin(z^n)| \leq 1$ for some $z \in \mathbb{C}$, and the Maclaurin expansion for the sine function is

$$|\sin(z^n)| = \left| \sum_{k=0}^{\infty} \frac{(-1)^k z^{n(2k+1)}}{(2k+1)!} \right| = |z^n| \left| \sum_{k=0}^{\infty} \frac{(-1)^k z^{2kn}}{(2k+1)!} \right| \geq |\omega||z^n|, \tag{2.3}$$

where $0 < |\omega| \leq 1$ except the values of $z \in \mathbb{C}$ for which $|\omega| = 0$ and satisfying the bound $\left| \sum_{k=0}^{\infty} \frac{(-1)^k z^{2kn}}{(2k+1)!} \right| \geq |\omega|$, (see the details [1]).

3. Escape criteria for the considered complex functions

In this section, we introduce the escape time algorithms via the viscosity approximation-type iterative method with s-convexity combination for novel complex function of the type $W(z) = \alpha e^{z^n} + \beta z^2 + \log \gamma^t$ and $T(z) = \sin(z^n) + \beta z^2 + \log \gamma^t$, where $n \geq 2,\ \alpha, \beta \in \mathbb{C}, \gamma \in \mathbb{C}\backslash\{0\}$ and $t \in \mathbb{R}, t \geq 1$. As a result, we establish a novel threshold escape radii and leverage them to visualize some non-classical variants of classical fractals, as illustrated in the subsequent outcomes.

3.1. *Escape criterion for* $\mathbf{W(z) = \alpha e^{z^n} + \beta z^2 + \log \gamma^t}$

In this subsection, we prove the escape criteria for transcendental function $W(z) = \alpha e^{z^n} + \beta z^2 + \log \gamma^t$, where $n \geq 2$, $\alpha, \beta \in \mathbb{C}, \gamma \in \mathbb{C}\backslash\{0\}$ and $t \in \mathbb{R}, t \geq 1$. via viscosity approximation-type iterative method with s-convexity.

Theorem 3.1
Assume that $z_0 \in \mathbb{C}$, $|z_0| \geq \max\{|\gamma|, |b|\} > \left(\dfrac{(2+s\mu)}{(1-s\mu)(1-s\nu)\big(|\gamma|^{n-2}-|\beta|\big)} + \dfrac{|\eta|}{\big(|\gamma|^{n-2}-|\beta|\big)} \right)$ and $|z_0^n| \leq |\alpha|(Re(z_0^n))$, where $\mu, \nu, |\omega| \in (0,1)$ and $|\gamma|^{n-2} - |\beta| \neq 0$. If the sequence $\{z_k\}_{k=0}^{\infty}$ is a viscosity approximation-type iterative method with s-convexity defined as

$$\begin{cases} z_{k+1} = \mu^s p(z_k) + (1-\mu)^s y_k, \\ y_k = \nu^s z_k + (1-\nu)^s W(z_k), \end{cases} \tag{3.1}$$

where $p(z) = az + b$ is contraction mapping $a, b \in \mathbb{C}$ with $|a| < 1$, and $k \geq 0$. Then $|z_k| \to \infty$, as $k \to \infty$.

Proof
For $k = 0$, consider from (3.1)

$$\begin{aligned} |y_0| &= |\nu^s z_0 + (1-\nu)^s W(z_0)| \\ &= |\nu^s z_0 + (1-\nu)^s (\alpha e^{z_0^n} + \beta z_0^2 + \log \gamma^t)| \\ &= |\nu^s z_0 + (1-\nu)^s (\alpha e^{z_0^n} + \beta z_0^2 + \eta\gamma)| \\ &\geq (1-\nu)^s |(\alpha e^{z_0^n} + \beta z_0^2)| - (1-\nu)^s |\eta\gamma| - \nu^s |z_0|. \end{aligned}$$

Utilizing binomial expansion of $(1-\nu)^s$ up to linear terms of ν, and $\nu, s \in (0,1]$, so $\nu^s \geq s\nu$, we get

$$\begin{aligned} |y_0| &\geq (1-s\nu)|(\alpha e^{z_0^n} + \beta z_0^2)| - (1-s\nu)|\eta\gamma| - s\nu|z_0| \\ &\geq (1-s\nu)|\alpha e^{z_0^n}| - (1-s\nu)|\beta||z_0^2| - (1-s\nu)|\eta||\gamma| - s\nu|z_0|, \quad |z_0| \geq |\gamma| \\ &\geq (1-s\nu)|\alpha||e^{Re(z_0^n)}| - (1-s\nu)|\beta||z_0^2| - (1-s\nu)|\eta||z_0| - s\nu|z_0|, \quad s\nu < 1 \\ &\geq (1-s\nu)|\alpha|Re(z_0^n) - (1-s\nu)|\beta||z_0^2| - (1-s\nu)|\eta||z_0| - |z_0|, \quad |z_0^n| \leq |\alpha|Re(z_0^n) \\ &\geq (1-s\nu)|z_0^n| - (1-s\nu)|\beta||z_0^2| - (1-s\nu)|\eta||z_0| - |z_0| \\ &\geq (1-s\nu)|z_0^2|\big(|z_0^{n-2}| - |\beta|\big) - (1-s\nu)|\eta||z_0| - |z_0|, \quad |z_0| \geq |\gamma| \\ &\geq |z_0|\Big((1-s\nu)|z_0|\big(|\gamma|^{n-2} - |\beta|\big) - (1-s\nu)|\eta| - 1\Big). \end{aligned} \tag{3.2}$$

From (3.1), consider

$$\begin{aligned} |z_1| &= |\mu^s p(z_0) + (1-\mu)^s y_0| \\ &= |\mu^s (az_0 + b) + (1-\mu)^s y_0| \\ &\geq (1-\mu)^s |y_0| - \mu^s |(az_0 + b)| \\ &\geq (1-\mu)^s |y_0| - \mu^s |az_0| - \mu^s |b|. \end{aligned}$$

Utilizing binomial expansion of $(1-\nu)^s$ up to linear terms of ν, and $\nu, s \in (0,1]$, so $\nu^s \geq s\nu$, we get

$$|z_1| \geq (1-s\mu)|y_0| - s\mu|a||z_0| - s\mu|b|$$

Using (3.2), and our assumption $|z_0| \geq \max\{|\gamma|, |b|\}$ yields that $-|b| \geq -|z_0|$, we have

$$\begin{aligned} |z_1| &\geq (1-s\mu)|z_0|\Big((1-s\nu)|z_0|\big(|\gamma|^{n-2} - |\beta|\big) - (1-s\nu)|\eta| - 1\Big) - s\mu|a||z_0| - s\mu|z_0| \\ &\geq (1-s\mu)|z_0|\Big((1-s\nu)|z_0|\big(|\gamma|^{n-2} - |\beta|\big) - (1-s\nu)|\eta| - 1\Big) - 2s\mu|z_0|, \quad |a| < 1 \\ &\geq |z_0|\Big((1-s\mu)(1-s\nu)|z_0|\big(|\gamma|^{n-2} - |\beta|\big) - (1-s\mu)(1-s\nu)|\eta| - s\mu - 1\Big), \end{aligned}$$

Since, $|z_0| \geq \max\{|c|, |b|\} > \left(\dfrac{|\eta|}{\big(|\gamma|^{n-2} - |\beta|\big)} + \dfrac{(2+s\mu)}{(1-s\mu)(1-s\nu)\big(|\gamma|^{n-2} - |\beta|\big)} \right)$, which implies $(1-s\mu)(1-s\nu)|z_0|\big(|\gamma|^{n-2} - |\beta|\big) - (1-s\mu)(1-s\nu)|\eta| - s\mu - 1 > 1$.

Hence $|z_1| > |z_0|$, which implies that there exists a real number $\Omega > 0$ so that $|z_1| > (1+\Omega)|z_0|$. On continuing the above procedure, we obtain $|z_k| > (1+\Omega)^k|z_0|$. Hence, $|z_k| \to \infty$, as $n \to \infty$. □

In the proof of Theorem 3.1, we have used only the fact that $|z_0| > \left(\frac{|\eta|}{\left(|\gamma|^{n-2}-|\beta|\right)} + \frac{(2+s\mu)}{(1-s\mu)(1-s\nu)\left(|\gamma|^{n-2}-|\beta|\right)}\right)$ and $|z_0| \geq \max\{|\gamma|, |b|\}$. So, we can refine it and obtain the following corollary.

Corollary 3.1
Let $|z_0| > \max\left\{|\gamma|, |b|, \left(\frac{|\eta|}{\left(|\gamma|^{n-2}-|\beta|\right)} + \frac{(2+s\mu)}{(1-s\mu)(1-s\nu)\left(|\gamma|^{n-2}-|\beta|\right)}\right)\right\}$ with $|\gamma|^{n-2} - |\beta| \neq 0$ and $|z_0^n| \leq |\alpha| Re(z_0^n))$, where $n \geq 2$, $\alpha, \beta \in \mathbb{C}, \gamma \in \mathbb{C}\backslash\{0\}$, $t \in \mathbb{R}, t \geq 1$, and $\mu, \nu \in (0,1)$, and $s \in (0,1]$ with $|a| < 1$. Then $|z_k| \to \infty$, as $n \to \infty$.

3.2. *Escape criterion for* $\mathbf{T(z) = \sin(z^n) + \beta z^2 + \log \gamma^t}$

In this subsection, we prove the escape criteria for transcendental function $T(z) = \sin(z^n) + \beta z^2 + \log \gamma^t$, where $n \geq 2$, $\beta \in \mathbb{C}, \gamma \in \mathbb{C}\backslash\{0\}$ and $t \in \mathbb{R}, t \geq 1$. via viscosity approximation-type iterative method with s-convexity.

Theorem 3.2
Assume that $z_0 \in \mathbb{C}$, $|z_0| \geq \max\{|\gamma|, |b|\} > \left(\frac{(2+s\mu)}{(1-s\mu)(1-s\nu)|\omega|\left(|\gamma|^{n-2}-|\beta|\right)} + \frac{|\eta|}{|\omega|\left(|\gamma|^{n-2}-|\beta|\right)}\right)$, where $\mu, \nu, |\omega| \in (0,1)$ and $|\gamma|^{n-2} - |\beta| \neq 0$. If the sequence $\{z_k\}$ is a viscosity approximation-type iterative method with s-convexity defined as

$$\begin{cases} z_{k+1} = \mu^s p(z_k) + (1-\mu)^s y_k, \\ y_k = \nu^s z_k + (1-\nu)^s T(z_k), \end{cases} \tag{3.3}$$

where $p(z) = az + b$ is contraction mapping $a, b \in \mathbb{C}$ with $|a| < 1$, and $k \geq 0$. Then $|z_k| \to \infty$, as $k \to \infty$.

Proof
For $k = 0$, consider from (3.3)

$$\begin{aligned} |y_0| &= |\nu^s z_0 + (1-\nu)^s T(z_0)| \\ &= |\nu^s z_0 + (1-\nu)^s(\sin(z_0^n) + \beta z_0^2 + \log \gamma^t)| \\ &= |\nu^s z_0 + (1-\nu)^s(\sin(z_0^n) + \beta z_0^2 + \eta\gamma)| \\ &\geq |(1-\nu)^s \sin(z_0^n)| - |(1-\nu)^s \beta z_0^2| - |(1-\nu)^s \eta\gamma| - |\nu^s z_0|. \end{aligned}$$

Utilizing binomial expansion of $(1-\nu)^s$ up to linear terms of $\nu, \nu \in (0,1)$ and $s \in (0,1]$, so $\nu^s \geq s\nu$, we get

$$\begin{aligned} |y_0| &\geq (1-s\nu)|\sin(z_0^n)| - (1-s\nu)|\beta z_0^2| - (1-s\nu)|\eta\gamma| - s\nu|z_0| \\ &\geq (1-s\nu)|\omega||z_0^n| - (1-s\nu)|\beta||z_0^2| - (1-s\nu)|\eta||z_0| - s\nu|z_0|, \ \ |z_0| \geq |\gamma| \\ &\geq (1-s\nu)|\omega||z_0^n| - (1-s\nu)|\beta||z_0^2| - (1-s\nu)|\eta||z_0| - |z_0|, \ \ s\nu < 1 \\ &\geq |z_0|\Big((1-s\nu)|z_0||\omega|(|z_0^{n-2}| - |\beta|) - (1-s\nu)|\eta| - 1\Big), \ \ |z_0| \geq |\gamma| \\ &\geq |z_0|\Big((1-s\nu)|z_0||\omega|(|\gamma|^{n-2} - |\beta|) - (1-s\nu)|\eta| - 1\Big). \end{aligned} \tag{3.4}$$

From (3.3), consider

$$\begin{aligned} |z_1| &= |\mu^s p(z_0) + (1-\mu)^s y_0| \\ &= |\mu^s(az_0+b) + (1-\mu)^s y_0| \\ &\geq (1-\mu)^s|y_0| - \mu^s|(az_0+b)| \\ &\geq (1-\mu)^s|y_0| - \mu^s|az_0| - \mu^s|b| \end{aligned}$$

Utilizing binomial expansion of $(1-\nu)^s$ up to linear terms of $\nu, \nu \in (0,1)$ and $s \in (0,1]$, so $\nu^s \geq s\nu$, we get

$$|z_1| \geq (1-s\mu)|y_0| - s\mu|a||z_0| - s\mu|b|.$$

Using (3.4), and our assumption $|z_0| \geq \max\{|\gamma|, |b|\}$ yields that $-|b| \geq -|z_0|$, we have

$$\begin{aligned} |z_1| &\geq (1-s\mu)|z_0|\Big((1-s\nu)|\omega||z_0|\big(|\gamma|^{n-2} - |\beta|\big) - (1-s\nu)|\eta| - 1\Big) - s\mu|a||z_0| - s\mu|z_0| \\ &\geq (1-s\mu)|z_0|\Big((1-s\nu)|\omega||z_0|\big(|\gamma|^{n-2} - |\beta|\big) - (1-s\nu)|\eta| - 1\Big) - 2s\mu|z_0|, \ |a| < 1 \\ &\geq |z_0|\Big((1-s\mu)(1-s\nu)|\omega||z_0|\big(|\gamma|^{n-2} - |\beta|\big) - (1-s\mu)(1-s\nu)|\eta| - s\mu - 1\Big), \end{aligned}$$

Since, $|z_0| \geq \max\{|\gamma|, |b|\} > \left(\dfrac{|\eta|}{|\omega|\big(|\gamma|^{n-2} - |\beta|\big)} + \dfrac{(2+s\mu)}{(1-s\mu)(1-s\nu)|\omega|\big(|\gamma|^{n-2} - |\beta|\big)}\right)$, which implies $(1-s\mu)(1-s\nu)|\omega||z_0|\big(|\gamma|^{n-2} - |\beta|\big) - (1-s\mu)(1-s\nu)|\eta| - s\mu - 1 > 1$.
Hence $|z_1| > |z_0|$, which implies that there exists a real number $\Omega > 0$ so that $|z_1| > (1+\Omega)|z_0|$. On continuing the above procedure, we obtain $|z_k| > (1+\Omega)^k|z_0|$. Hence, $|z_k| \to \infty$, as $n \to \infty$. □

In the proof of Theorem 3.2, we have used only the fact that $|z_0| > \left(\dfrac{|\eta|}{|\omega|\big(|\gamma|^{n-2} - |\beta|\big)} + \dfrac{(2+s\mu)}{(1-s\mu)(1-s\nu)|\omega|\big(|\gamma|^{n-2} - |\beta|\big)}\right)$ and $|z_0| \geq \max\{|\gamma|, |b|\}$. So, we can refine it and obtain the following corollary.

Corollary 3.2
Let $|z_0| > \max\left\{|\gamma|, |b|, \left(\dfrac{|\eta|}{|\omega|\big(|\gamma|^{n-2} - |\beta|\big)} + \dfrac{(2+s\mu)}{(1-s\mu)(1-s\nu)|\omega|\big(|\gamma|^{n-2} - |\beta|\big)}\right)\right\}$ with $|\gamma|^{n-2} - |\beta| \neq 0$, where $n \geq 2$, , $\beta \in \mathbb{C}, \gamma \in \mathbb{C}\backslash\{0\}$, $t \in \mathbb{R}, t \geq 1$, and $\mu, \nu \in (0,1)$ and $s, |\omega| \in (0,1]$ with $|a| < 1$. Then $|z_k| \to \infty$, as $n \to \infty$.

4. Application of Fractals

In this section, we tailor two algorithms: one for the Julia set of $W(z) = \alpha e^{z^n} + \beta z^2 + \log \gamma^t$ and the other for $T(z) = \sin(z^n) + \beta z^2 + \log \gamma^t$ employing the viscosity approximation-type iterative method with s-convexity, where $n \geq 2$, $\beta \in \mathbb{C}, \gamma \in \mathbb{C}\backslash 0$, and $t \in \mathbb{R}, t \geq 1$. We illustrate graphs of Julia sets at various input parameters, generating Julia sets through the viscosity approximation-type iterative method with s-convexity using Algorithm 1 and 2, and comparing the resultant images. Finally, we visualize Julia sets for various input parameters and different values of n. Throughout the paper, a maximum number of iterations $k = 100$ is consistently applied.

Algorithm 1 Geometry of Viscosity Julia set for $W(z) = \alpha e^{z^n} + \beta z^2 + \log \gamma^t$,

Input: $W(z) = \alpha e^{z^n} + \beta z^2 + \log \gamma^t$, where $n \geq 2$, $\alpha, \beta \in \mathbb{C}, \gamma \in \mathbb{C}\backslash\{0\}$ and $t \in \mathbb{R}, t \geq 1$; K-maximal number of iterations; A-area; $\mu, \nu \in (0,1)$; $p(z) = az + b$, where $a, b \in \mathbb{C}$ with $|a| < 1$; colourmap $[0..C\text{-}1]$-color with C colors.

Output: Julia set for area A

for $z_0 \in A$ **do**

$\eta = \frac{\log \gamma^t}{\gamma}$

$$R_1 = \max\left\{|\gamma|, |b|, \left(\frac{|\eta|}{\left(|\gamma|^{n-2} - |\beta|\right)} + \frac{(2+s\mu)}{(1-s\mu)(1-s\nu)\left(|\gamma|^{n-2} - |\beta|\right)}\right)\right\}$$

$R_2 = (|\alpha| Re(z_0^n))^{\frac{1}{n}}$

k=0

while $k \leq K$ **do**

$z_{k+1} = \mu^s p(z_k) + (1-\mu)^s y_k,$

$y_k = \nu^s z_k + (1-\nu)^s W(z_k)$

if $R_1 < |z_{k+1}| \leq R_2$ then break

end if

k=k+1

$j = [(C-1)\frac{k}{K}]$

colour z_0 with colourmap $[j]$

Figure 1. Color map used in sketching the fractals.

Example 4.1

In this example, we present two cases. In the first case, we take an integer value of t, i.e., $t = 3, 6, 9$ and in the second one a non-integer value, i.e., $t = 0.5, 2.5, 6.5$. Note that the last column in all the tables displays the image execution time (in short, IET) in seconds. Julia sets for $W(z) = \alpha e^{z^n} + \beta z^2 + log\gamma^t$ via viscosity approximation-type iterative method with s-convexity are generated here with the following inputs:

Table 1 : Fixed value of γ as purely real and varying t.

	n	t	α	β	γ	a	b	μ	ν	s	IET (in sec)
(i)	2	3	0.2	0.6	9	0.8	0.3	0.8	0.7	0.85	$4.88s$
(ii)	2	6	0.2	0.6	9	0.8	0.3	0.8	0.7	0.85	$4.92s$
(iii)	2	9	0.2	0.6	9	0.8	0.3	0.8	0.7	0.85	$5.09s$
(iv)	2	0.5	0.2	0.6	9	0.8	0.3	0.8	0.7	0.85	$4.76s$
(v)	2	2.5	0.2	0.6	9	0.8	0.3	0.8	0.7	0.85	$4.82s$
(vi)	2	6.5	0.2	0.6	9	0.8	0.3	0.8	0.7	0.85	$4.97s$

In Figure 2, we fixed the value of γ to 9 (purely real) and varying the value of t, in the first case, we take an integer value of t, i.e., $t = 3, 6, 9$ (Figure 2 (i)-(iii)), and in the second one a non-integer value, i.e., $t = 0.5, 2.5, 6.5$ (Figure 2 (iv)-(vi)). From the images, we see that the Julia set becomes larger with the increase of the value of t. Thus, the value of t has a great impact on the shape, size and color to the fractals, and the generated Julia sets looks like flowers and Rangoli or may be compared to glass painting. We can see some spiral structures but the spiral pattern arms and the size of lashes of bunches slightly increase with the increase the value of t.

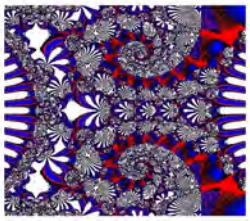

(i) $t = 3$

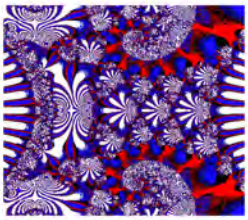

(ii) $t = 6$

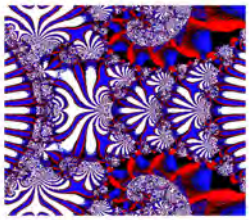

(iii) $t = 9$

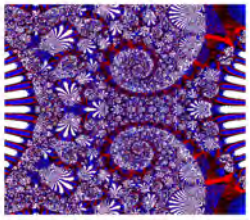

(iv) $t = 0.5$

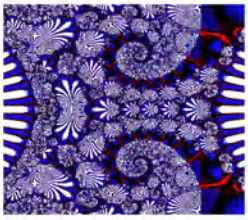

(v) $t = 2.5$

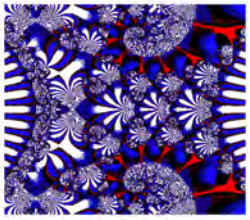

(vi) $t = 6.5$

Figure 2. Julia sets for $n = 2$ with $\gamma = 9$ and varying t.

Table 2 : Fixed value of γ as purely complex and varying t.

	n	t	α	β	γ	a	b	μ	ν	s	IET (in sec)
(i)	2	3	0.2	0.6	$6i$	0.8	0.3	0.8	0.7	0.85	$4.84s$
(ii)	2	6	0.2	0.6	$6i$	0.8	0.3	0.8	0.7	0.85	$5.57s$
(iii)	2	9	0.2	0.6	$6i$	0.8	0.3	0.8	0.7	0.85	$5.77s$
(iv)	2	0.5	0.2	0.6	$6i$	0.8	0.3	0.8	0.7	0.85	$3.74s$
(v)	2	2.5	0.2	0.6	$6i$	0.8	0.3	0.8	0.7	0.85	$4.80s$
(vi)	2	6.5	0.2	0.6	$6i$	0.8	0.3	0.8	0.7	0.85	$5.63s$

In Figure 3, we fixed the value of γ to $6i$ (purely imaginary) and varying the value of t. From the images, we see that the Julia set becomes larger with the increase of the value of t. Thus, the value of t has a significant impact on the shape, size and color to the fractals, and the generated Julia sets looks like flowers and Rangoli or may be compared to glass painting. We can see some spiral structures but the spiral pattern arms and the size of lashes of bunches slightly increase with the increase the value of t.

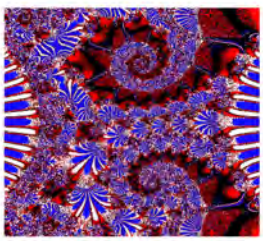

(i) $t = 3$

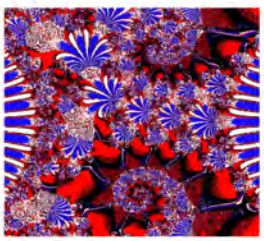

(ii) $t = 6$

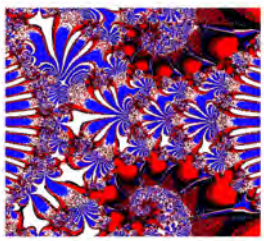

(iii) $t = 9$

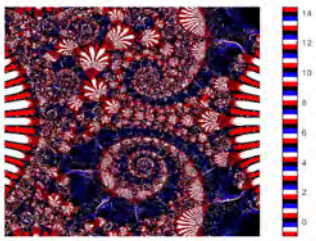

(iv) $t = 0.5$

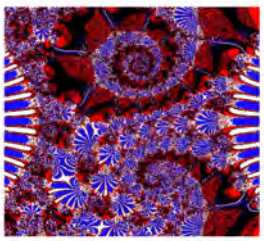

(v) $t = 2.5$

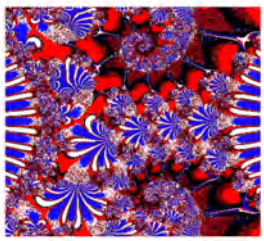

(vi) $t = 6.5$

Figure 3. Julia sets for $n = 2$ with $\gamma = 6i$ and varying t.

Table 3 : Fixed value of γ as complex and varying t.

	n	t	α	β	γ	a	b	μ	ν	s	IET (in sec)
(i)	2	3	0.2	0.6	$3+2i$	0.8	0.3	0.8	0.7	0.85	$4.74s$
(ii)	2	6	0.2	0.6	$3+2i$	0.8	0.3	0.8	0.7	0.85	$4.77s$
(iii)	2	9	0.2	0.6	$3+2i$	0.8	0.3	0.8	0.7	0.85	$5.17s$
(iv)	2	0.5	0.2	0.6	$3+2i$	0.8	0.3	0.8	0.7	0.85	$4.03s$
(v)	2	2.5	0.2	0.6	$3+2i$	0.8	0.3	0.8	0.7	0.85	$4.47s$
(vi)	2	6.5	0.2	0.6	$3+2i$	0.8	0.3	0.8	0.7	0.85	$4.84s$

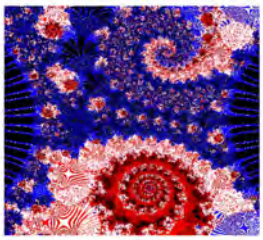

(i) $t = 3$

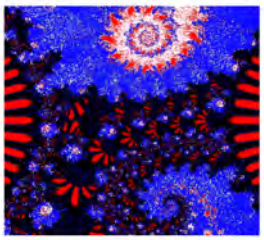

(ii) $t = 6$

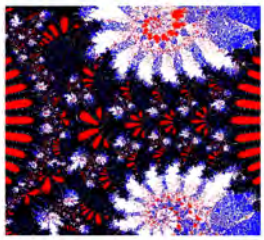

(iii) $t = 9$

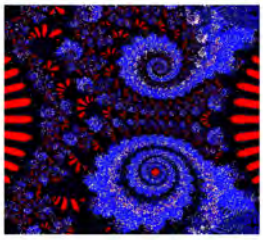

(iv) $t = 0.5$

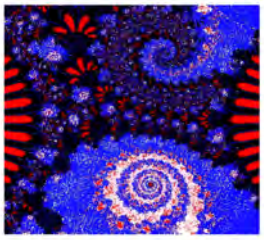

(v) $t = 2.5$

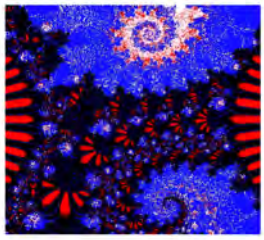

(vi) $t = 6.5$

Figure 4. Julia sets for $n = 2$ with $\gamma = 3 + 2i$ and varying t.

In Figure 4, we fixed the value of γ to $3+2i$ and varying the value of t. From the images, the value of t has a significant impact on the shape, size and color to the fractals, and the generated Julia sets looks like spiral galaxy, leaf of Rex Begonia and Rangoli or may be compared to glass painting. However, when we look closely, then we notice that, we can see some beautiful spiral structures and the spiral pattern arms slightly different with the increase the value of t. At first sight, the spiral arm in the lower in Figure $4(i,v)$, and the spiral arm in the upper in Figure $4(ii,vi)$, or the two spiral arms upper as well as lower in Figure $4(iii,iv)$ are slightly different from the other arms.

Table 4 : Fixed all the parameters values complex and varying t.

	n	t	α	β	γ	a	b	μ	ν	s	IET (in sec)
(i)	2	3	$-1.725-1.725i$	$-0.025+0.025i$	$-1.725-1.725i$	$0.018+0.4i$	$0.5+0.09i$	0.17	0.18	0.9	$6.12s$
(ii)	2	6	$-1.725-1.725i$	$-0.025+0.025i$	$-1.725-1.725i$	$0.018+0.4i$	$0.5+0.09i$	0.17	0.18	0.9	$6.87s$
(iii)	2	9	$-1.725-1.725i$	$-0.025+0.025i$	$-1.725-1.725i$	$0.018+0.4i$	$0.5+0.09i$	0.17	0.18	0.9	$7.87s$
(iv)	2	0.5	$-1.725-1.725i$	$-0.025+0.025i$	$-1.725-1.725i$	$0.018+0.4i$	$0.5+0.09i$	0.17	0.18	0.9	$4.94s$
(v)	2	2.5	$-1.725-1.725i$	$-0.025+0.025i$	$-1.725-1.725i$	$0.018+0.4i$	$0.5+0.09i$	0.17	0.18	0.9	$5.37s$
(vi)	2	6.5	$-1.725-1.725i$	$-0.025+0.025i$	$-1.725-1.725i$	$0.018+0.4i$	$0.5+0.09i$	0.17	0.18	0.9	$7.47s$

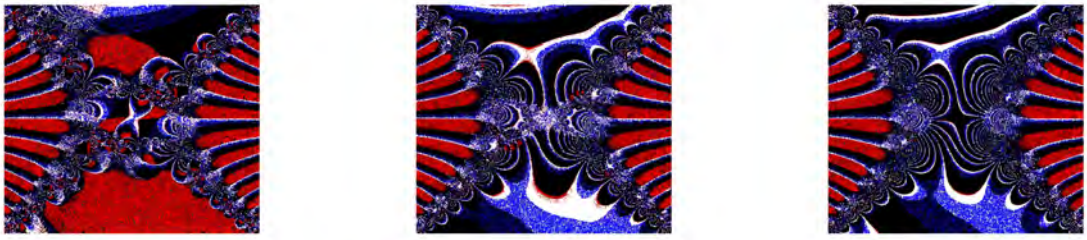

(i) $t=3$ (ii) $t=6$ (iii) $t=9$

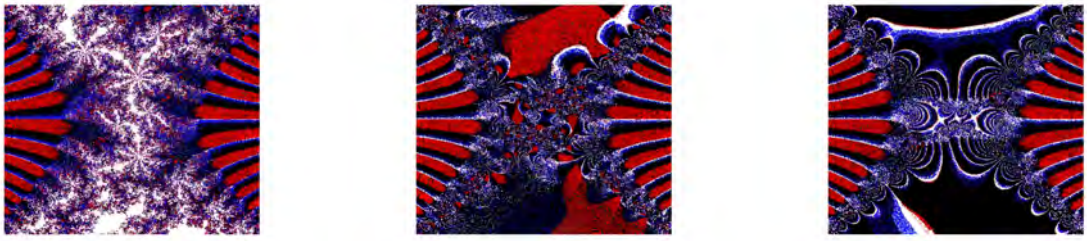

(iv) $t=0.5$ (v) $t=2.5$ (vi) $t=6.5$

Figure 5. Julia sets for $n=2$ with all the parameters values complex and varying t.

In Figure 5, we fixed all the parameters values are complex and varying the value of t. From the images, the value of t has a significant change on the shape, size and color to the fractals, and the generated Julia sets looks like leaf of Rex Begonia, spiral galaxy and Rangoli or may be compared to glass painting. Julia sets are slightly different with the increase the value of t. We notice that, the generated Julia set in Figure $5(iv)$ is different from the others. The image execution time consistently increases as the value of t rises, as shown in the last column of Table 5.

Table 5 : Fixed value of t and varying the parameters μ and ν.

	n	t	α	β	γ	a	b	μ	ν	s	IET (in sec)
(i)	2	5	0.2	0.6	3	0.8	0.3	0.1	0.1	0.85	$4.81s$
(ii)	2	5	0.2	0.6	3	0.8	0.3	0.3	0.3	0.85	$4.84s$
(iii)	2	5	0.2	0.6	3	0.8	0.3	0.7	0.7	0.85	$5.06s$
(iv)	2	5	0.2	0.6	3	0.8	0.3	0.9	0.9	0.85	$4.61s$
(v)	2	5	0.2	0.6	3	0.8	0.3	0.1	0.8	0.85	$4.72s$
(vi)	2	5	0.2	0.6	3	0.8	0.3	0.8	0.1	0.85	$4.79s$

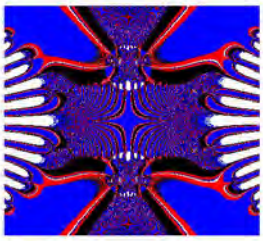

(i) $\mu = 0.1$ and $\nu = 0.1$

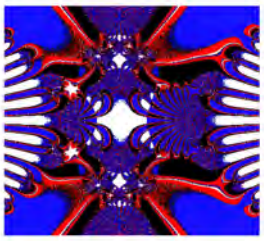

(ii) $\mu = 0.3$ and $\nu = 0.3$

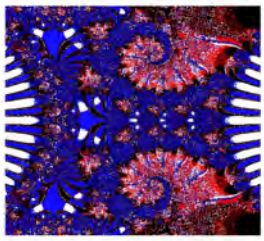

(iii) $\mu = 0.7$ and $\nu = 0.7$

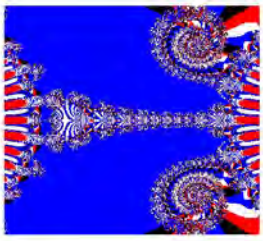

(iv) $\mu = 0.9$ and $\nu = 0.9$

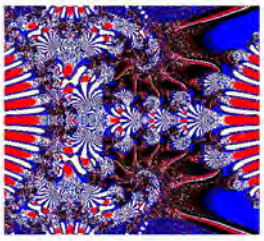

(v) $\mu = 0.1$ and $\nu = 0.8$

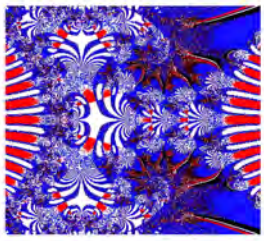

(vi) $\mu = 0.8$ and $\nu = 0.1$

Figure 6. Julia sets for $n = 2$ with $t = 5$, and varying μ and ν.

In Figure 6, we fixed all the parameters values and changed the values of μ and ν. From the images, the values of μ and ν have the significant changes on the shape, size and color to the fractals, and the generated Julia sets looks like leaf of Rex Begonia, spiral galaxy or may be compared to glass painting. We notice that, the generated Julia set in Figure 6(i, ii) are sightly same, the sets in Figure 6(v, vi) are sightly same, the set in Figure 6(iii) and Figure 6(iv) are different from the others for different vales of μ and ν. The image execution time is strictly increase with the increase the value of t which is given in the last column in Table 6.

Table 6 : Effect of change in the value of s.

	n	t	α	β	γ	a	b	μ	ν	s	IET (in sec)
(i)	2	5	0.23	1.8	3	0.8	0.3	0.85	0.75	0.1	$4.31s$
(ii)	2	5	0.23	1.8	3	0.8	0.3	0.85	0.75	0.3	$4.56s$
(iii)	2	5	0.23	1.8	3	0.8	0.3	0.85	0.75	0.5	$4.71s$
(iv)	2	5	0.23	1.8	3	0.8	0.3	0.85	0.75	0.7	$4.84s$
(v)	2	5	0.23	1.8	3	0.8	0.3	0.85	0.75	0.9	$4.97s$
(vi)	2	5	0.23	1.8	3	0.8	0.3	0.85	0.75	1	$5.11s$

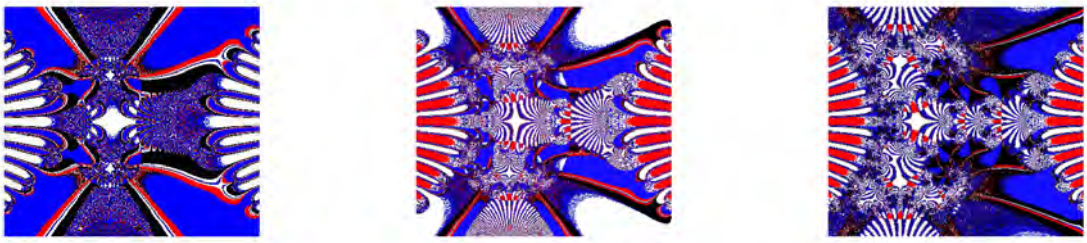

(i) $s = 0.1$ (ii) $s = 0.3$ (iii) $s = 0.5$

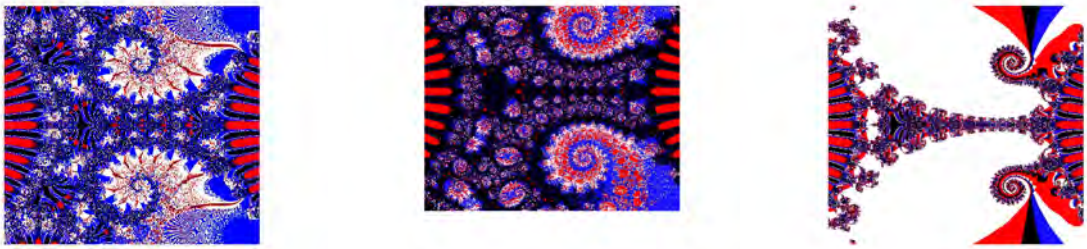

(iv) $s = 0.7$ (v) $s = 0.9$ (vi) $s = 1$

Figure 7. Julia sets for $n = 2$ with $t = 5$ and varying s.

In Figure 7, we fixed all the parameters values and varying the value of s. From the images, the value of s has a significant change on the shape, size and color to the fractals, and the generated Julia sets looks like spiral galaxy, leaf of Rex Begonia and Rangoli or may be compared to glass painting. Julia sets are slightly different with the increase the value of s. However, when we look closely, then we notice that, we can see some beautiful spiral structures and the spiral pattern arms slightly different in Figure $7(iv, v)$, t or the two spiral arms upper as well as lower in Figure $7(vi)$, the sets in Figure $7(i, ii)$ and Figure $7(ii)$ are different from the other. The image execution time consistently increases as the value of t rises, as shown in the last column of Table 7.

Table 7 : Effect of the value of n.

	n	t	α	β	γ	a	b	μ	ν	s	IET (in sec)
(i)	3	5	3	0.91	9	0.8	0.35	0.8	0.9	0.85	$6.86s$
(ii)	5	5	3	0.91	9	0.8	0.35	0.8	0.9	0.85	$7.23s$
(iii)	7	5	3	0.91	9	0.8	0.35	0.8	0.9	0.85	$7.97s$
(iv)	11	5	3	0.91	9	0.8	0.35	0.8	0.9	0.85	$8.87s$
(v)	23	5	3	0.91	9	0.8	0.35	0.8	0.9	0.85	$11.78s$
(vi)	2001	5	3	0.91	9	0.8	0.35	0.8	0.9	0.85	$14.53s$

In Figure 8, we fixed all the parameters values and varying the value of n. From the images, the value of n has a significant change on the shape, size and color to the fractals. The generated Julia sets have different patterns with the increase the value of n. The image execution time consistently increases as the value of n rises, as shown in the last column of Table 8.

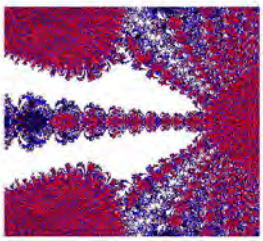

(i) $n = 3$

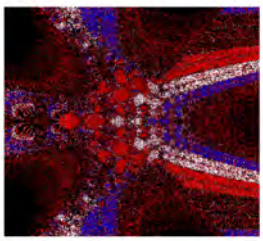

(ii) $n = 5$

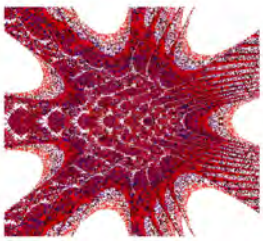

(iii) $n = 7$

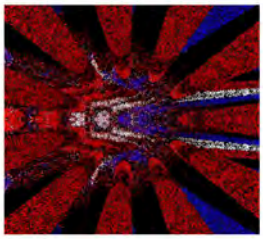

(iv) $n = 11$

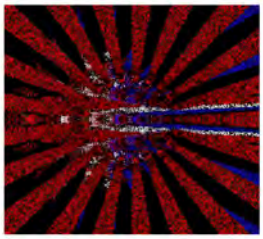

(v) $n = 23$

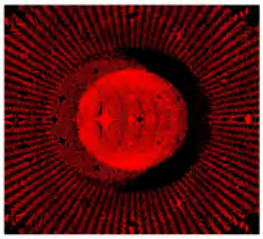

(vi) $n = 2001$

Figure 8. Julia sets for $n = 2$ with $t = 5$ and varying n.

Algorithm 2 Geometry of Viscosity Julia set for $T(z) = \sin(z^n) + \beta z^2 + \log \gamma^t$

Input: $T(z) = \sin(z^n) + \beta z^2 + \log \gamma^t$, where $n \geq 2$, $\beta \in \mathbb{C}, \gamma \in \mathbb{C}\backslash\{0\}$ and $t \in \mathbb{R}, t \geq 1$; K-maximal number of iterations; A-area; $|\omega|, s \in (0, 1]$; $p(z) = az + b$, where $a, b \in \mathbb{C}$ and $|a| < 1$; colourmap $[0..C\text{-}1]$-color with C colors.

Output: Julia set for area A

for $z_0 \in A$ **do**

$\eta = \frac{\log \gamma^t}{\gamma}$

$$R = \max\left\{|\gamma|, |b|, \left(\frac{|\eta|}{|\omega|\big(|c|^{n-2} - |\beta|\big)} + \frac{(2 + s\mu)}{(1 - s\mu)(1 - s\nu)|\omega|\big(|c|^{n-2} - |\beta|\big)}\right)\right\}$$

with $|\gamma|^{n-2} - |\beta| \neq 0$

k=0

while $k \leq K$ **do**

$z_{k+1} = \mu^s p(z_k) + (1 - \mu)^s y_k$,

$y_k = \nu^s z_k + (1 - \nu)^s W(z_k)$

if $|z_{k+1}| > R$ then

break

end if

k=k+1

$j = [(C - 1)\frac{k}{K}]$

colour z_0 with colourmap $[j]$

Example 4.2

In this example, we present two cases. In the first case, we take an integer value of t, i.e., $t = 3, 6, 9$ and in the second one a non-integer value, i.e., $t = 0.5, 2.5, 6.5$. Note that the last column in all the tables displays

the image execution time (in short, IET) in seconds. Julia sets for $T(z) = \sin(z^n) + \beta z^2 + \log \gamma^t$ via viscosity approximation-type iterative method with s-convexity are generated here with the following inputs:

Table 8 : Fixed value of γ as purely real and varying t.

	n	t	β	γ	a	b	μ	ν	s	IET (in sec)
(i)	3	3	0.3	3	0.8	0.3	0.8	0.7	0.85	$4.76s$
(ii)	3	6	0.3	3	0.8	0.3	0.8	0.7	0.85	$4.81s$
(iii)	3	9	0.3	3	0.8	0.3	0.8	0.7	0.85	$4.71s$
(iv)	3	0.5	0.3	3	0.8	0.3	0.8	0.7	0.85	$4.07s$
(v)	3	2.5	0.3	3	0.8	0.3	0.8	0.7	0.85	$4.49s$
(vi)	3	11.5	0.3	3	0.8	0.3	0.8	0.7	0.85	$5.11s$

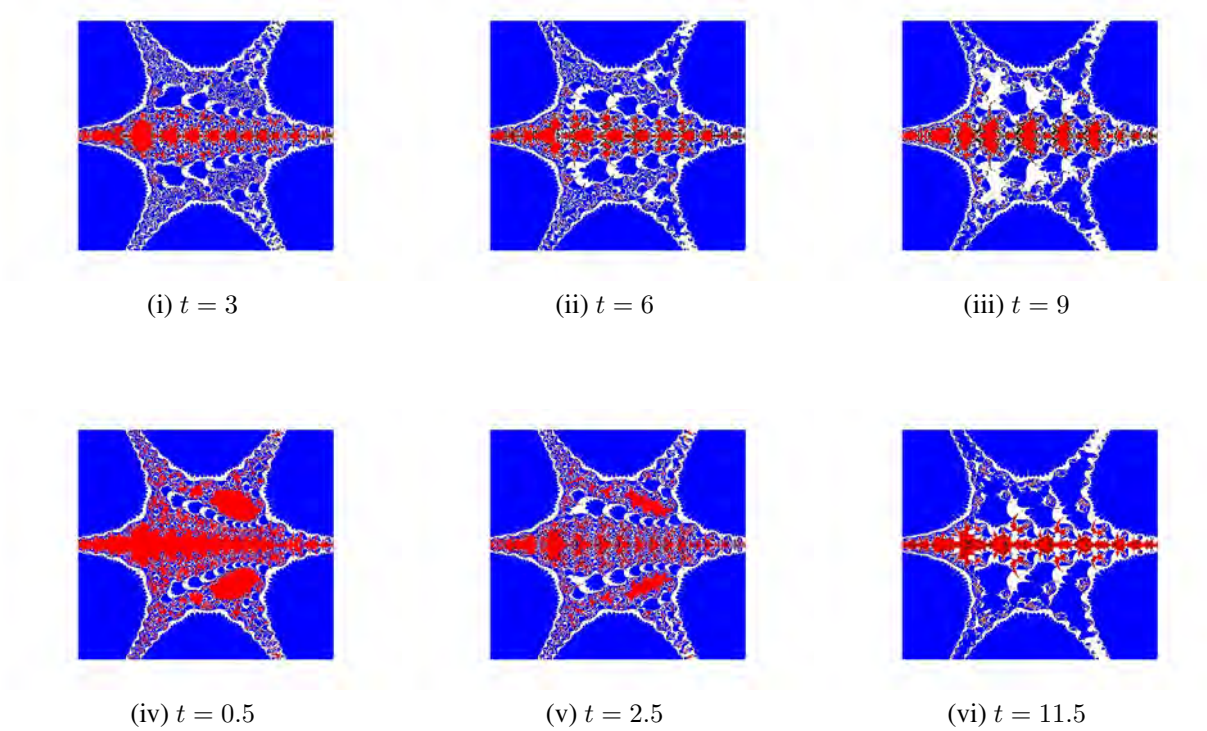

(i) $t = 3$ (ii) $t = 6$ (iii) $t = 9$

(iv) $t = 0.5$ (v) $t = 2.5$ (vi) $t = 11.5$

Figure 9. Julia sets for $n = 2$ with $\gamma = 9, |\omega| = 0.35$, and varying t.

Table 9 : Fixed the value γ as purely imaginary and varying t.

	n	t	β	γ	a	b	μ	ν	s	IET (in sec)
(i)	3	3	0.3	$1.5i$	0.8	0.3	0.8	0.7	0.85	$4.49s$
(ii)	3	6	0.3	$1.5i$	0.8	0.3	0.8	0.7	0.85	$4.61s$
(iii)	3	9	0.3	$1.5i$	0.8	0.3	0.8	0.7	0.85	$4.71s$
(iv)	3	0.5	0.3	$1.5i$	0.8	0.3	0.8	0.7	0.85	$4.27s$
(v)	3	2.5	0.3	$1.5i$	0.8	0.3	0.8	0.7	0.85	$4.43s$
(vi)	3	11.5	0.3	$1.5i$	0.8	0.3	0.8	0.7	0.85	$4.88s$

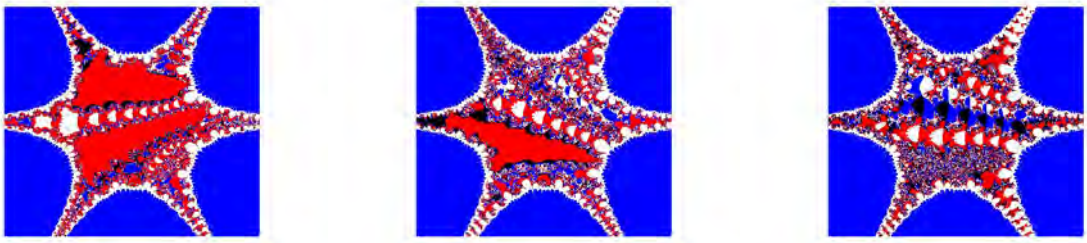

(i) $t = 3$ (ii) $t = 6$ (iii) $t = 9$

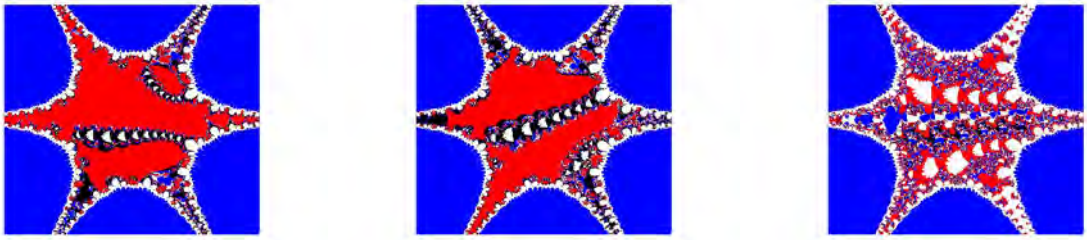

(iv) $t = 0.5$ (v) $t = 2.5$ (vi) $t = 6.5$

Figure 10. Julia sets for $n = 2$ with $\gamma = 6i$, $|\omega| = 0.65$, and varying t.

All Julia sets for $n = 3$ have six bunches of lashes. From six bunches of lashes, three are symmetrical to x-axis and other three are symmetrical to y-axis. The main body shape changed slightly while the parameters are changing. In Figure 9-10, we fixed all the parameters values and varying the value of γ and t, and all the figures look similar to each other but have difference in Julia points and the angle between every two bunches is $\frac{\pi}{3}$. From the images, the different value of the parameters have a significant change on the shape, size and color to the fractals and more beauty is added to the symmetrical pattern. The image execution time consistently increases as the value of t rises, as shown in the last column of Table 9.

Table 10 : Fixed value of γ as complex and varying t.

	n	t	β	γ	a	b	μ	ν	s	IET (in sec)
(i)	3	3	0.3	$1.5i$	0.8	0.3	0.8	0.7	0.85	$4.87s$
(ii)	3	6	0.3	$1.5i$	0.8	0.3	0.8	0.7	0.85	$5.03s$
(iii)	3	9	0.3	$1.5i$	0.8	0.3	0.8	0.7	0.85	$5.41s$
(iv)	3	0.5	0.3	$1.5i$	0.8	0.3	0.8	0.7	0.85	$4.37s$
(v)	3	2.5	0.3	$1.5i$	0.8	0.3	0.8	0.7	0.85	$4.63s$
(vi)	3	11.5	0.3	$1.5i$	0.8	0.3	0.8	0.7	0.85	$5.88s$

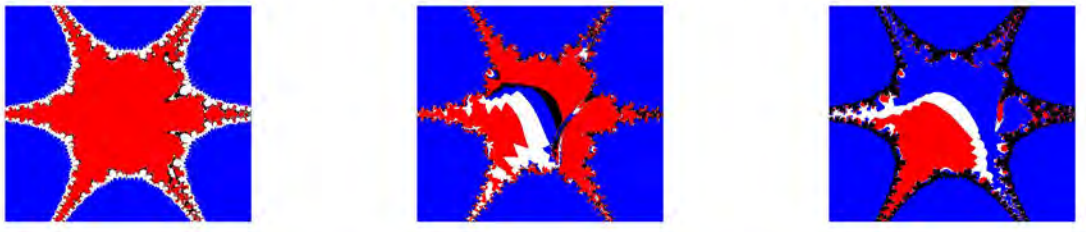

(i) $t = 3$ (ii) $t = 6$ (iii) $t = 9$

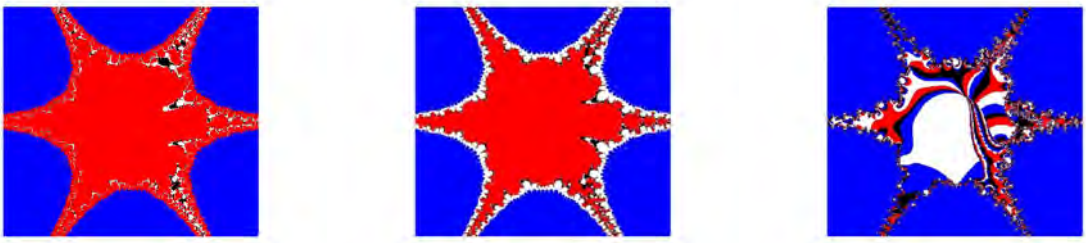

(iv) $t = 0.5$ (v) $t = 2.5$ (vi) $t = 6.5$

Figure 11. Julia sets for $n = 2$ with $\gamma = 3 + 2i$, $|\omega| = 0.15$, and varying t.

Table 11 : Fixed all the parameters values complex and varying t.

	n	t	β	γ	a	b	μ	ν	s	IET (in sec)
(i)	3	3	$-0.025 + 0.025i$	$0.75 - 0.75i$	$0.018 + 0.04i$	$0.005 + 0.01i$	0.8	0.7	0.85	$4.79s$
(ii)	3	6	$-0.025 + 0.025i$	$0.75 - 0.75i$	$0.018 + 0.04i$	$0.005 + 0.01i$	0.8	0.7	0.85	$5.19s$
(iii)	3	9	$-0.025 + 0.025i$	$0.75 - 0.75i$	$0.018 + 0.04i$	$0.005 + 0.01i$	0.8	0.7	0.85	$5.59s$
(iv)	3	0.5	$-0.025 + 0.025i$	$0.75 - 0.75i$	$0.018 + 0.04i$	$0.005 + 0.01i$	0.8	0.7	0.85	$4.19s$
(v)	3	2.5	$-0.025 + 0.025i$	$0.75 - 0.75i$	$0.018 + 0.04i$	$0.005 + 0.01i$	0.8	0.7	0.85	$4.69s$
(vi)	3	11.5	$-0.025 + 0.025i$	$0.75 - 0.75i$	$0.018 + 0.04i$	$0.005 + 0.01i$	0.8	0.7	0.85	$6.13s$

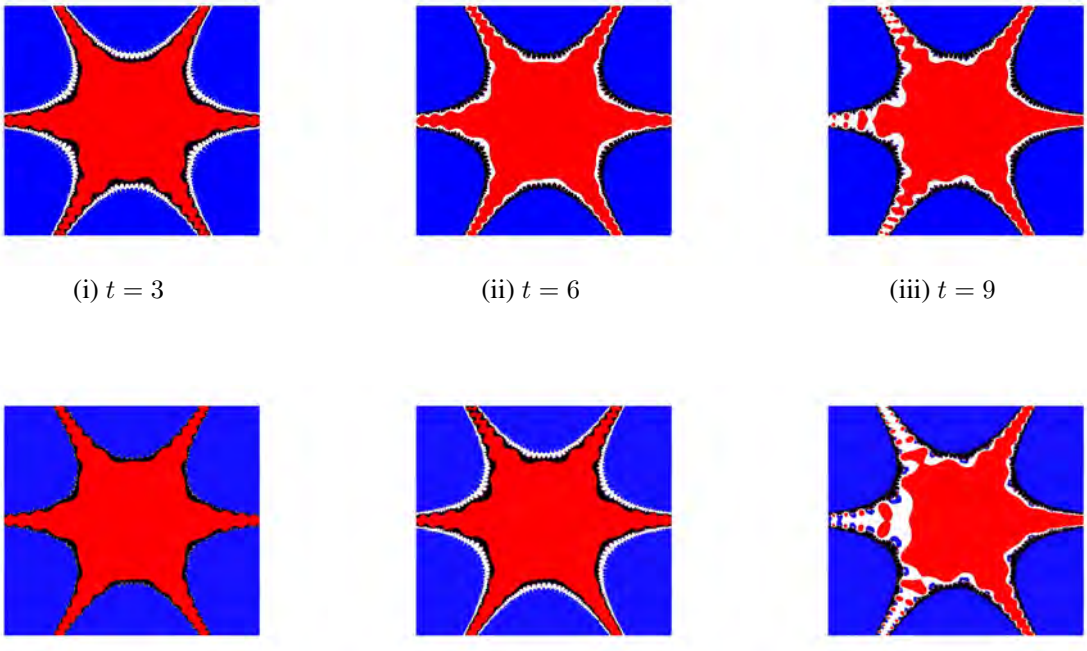

(i) $t = 3$ (ii) $t = 6$ (iii) $t = 9$

(iv) $t = 0.5$ (v) $t = 2.5$ (vi) $t = 11.5$

Figure 12. Julia sets for $n = 2$ with all the parameters values complex and varying t.

Table 12 : Effect of change in the values of t, μ and ν.

	n	t	β	γ	a	b	μ	ν	s	IET (in sec)
(i)	3	3	0.3	3	0.8	0.3	0.1	0.1	0.85	$4.97s$
(ii)	3	6	0.3	3	0.8	0.3	0.3	0.3	0.85	$5.21s$
(iii)	3	9	0.3	3	0.8	0.3	0.7	0.7	0.85	$5.61s$
(iv)	3	0.5	0.3	3	0.8	0.3	0.9	0.9	0.85	$4.77s$
(v)	3	2.5	0.3	3	0.8	0.3	0.1	0.9	0.85	$4.83s$
(vi)	3	11.5	0.3	3	0.8	0.3	0.9	0.1	0.85	$5.88s$

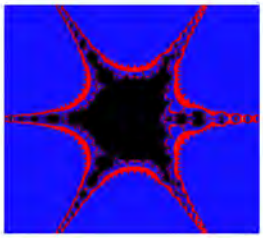

(i) $\mu = 0.1$ and $\nu = 0.1$

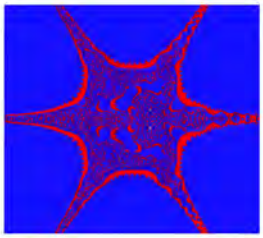

(ii) $\mu = 0.3$ and $\nu = 0.3$

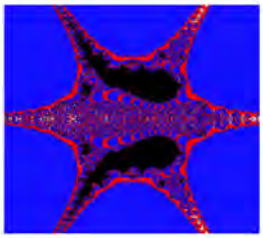

(iii) $\mu = 0.7$ and $\nu = 0.7$

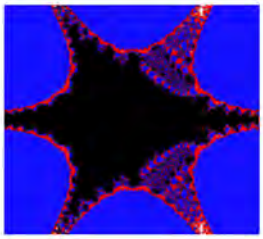

(iv) $\mu = 0.9$ and $\nu = 0.9$

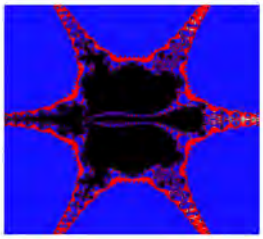

(v) $\mu = 0.1$ and $\nu = 0.8$

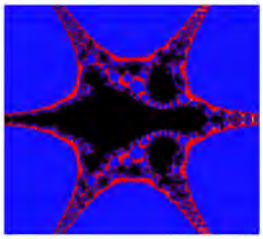

(vi) $\mu = 0.8$ and $\nu = 0.1$

Figure 13. Julia sets for $n = 2$ with $t = 5, |\omega| = 0.55$, and varying the parameters μ and ν.

Table 13 : Effect of change in the values of t and s.

	n	t	β	γ	a	b	μ	ν	s	IET (in sec)
(i)	3	3	0.3	3	0.8	0.3	0.1	0.1	0.1	$4.79s$
(ii)	3	6	0.3	3	0.8	0.3	0.3	0.3	0.3	$4.86s$
(iii)	3	9	0.3	3	0.8	0.3	0.7	0.7	0.5	$4.91s$
(iv)	3	0.5	0.3	3	0.8	0.3	0.9	0.9	0.7	$4.67s$
(v)	3	2.5	0.3	3	0.8	0.3	0.1	0.9	0.9	$4.76s$
(vi)	3	11.5	0.3	3	0.8	0.3	0.9	0.1	1	$4.97s$

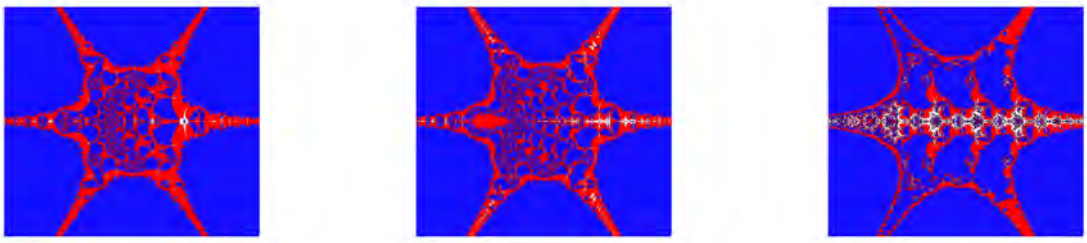

(i) $s = 0.1$ (ii) $s = 0.3$ (iii) $s = 0.5$

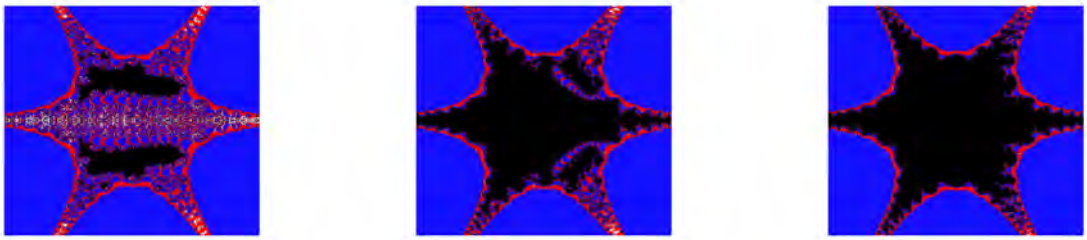

(iv) $s = 0.7$ (v) $s = 0.9$ (vi) $s = 1$

Figure 14. Julia sets for $n = 3$, and varying the parameters t and s.

Table 14: Effect of the value of n.

	n	t	β	γ	a	b	μ	ν	s	IET (in sec)
(i)	2	5	0.3	3	0.8	0.3	0.1	0.1	0.1	$6.39s$
(ii)	5	5	0.3	3	0.8	0.3	0.3	0.3	0.3	$6.69s$
(iii)	7	5	0.3	3	0.8	0.3	0.7	0.7	0.5	$7.48s$
(iv)	11	5	0.3	3	0.8	0.3	0.9	0.9	0.7	$7.69s$
(v)	23	5	0.3	3	0.8	0.3	0.1	0.9	0.9	$7.93s$
(vi)	2001	5	0.3	3	0.8	0.3	0.9	0.1	1	$12.31s$

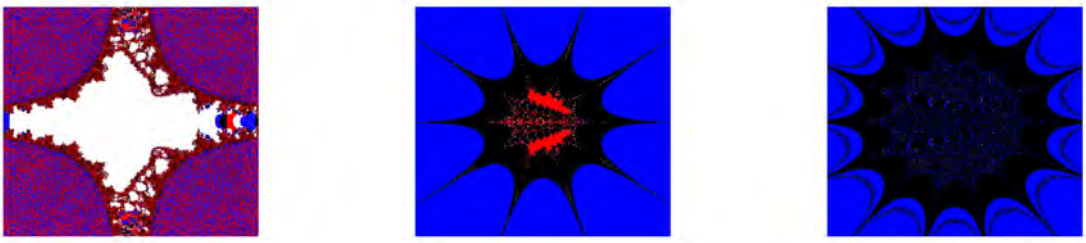

(i) $n = 2$ (ii) $n = 5$ (iii) $n = 7$

The size of lashes gradually decreases from the center of the bunch and the angle between every two bunches is $\frac{K\pi}{n}$, where K represented the positions of attractors from the initial attractor and same argument for Julia set with an extra characteristic that image of Julia sets contains n type of Julia set at center for every n.

All Julia sets for $n = 3$ have six bunches of lashes. Among these, three are symmetrical to the x-axis and the other three are symmetrical to the y-axis. The main body shape changes slightly as the parameters vary. The size

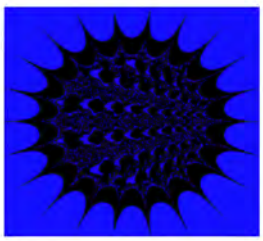

(iv) $n = 11$

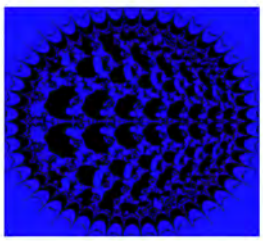

(v) $n = 23$

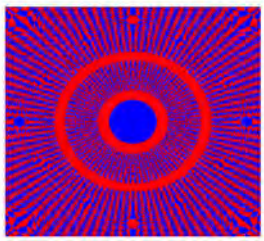

(vi) $n = 2001$

Figure 15. Julia sets for $n = 3$ with $t = 5$, $|\omega| = 0.85$, and varying n.

of the lashes gradually decreases from the center of the bunch, and the angle between every two bunches is $\frac{\pi}{3}$. In Figures 9-15, all the figures look similar to each other but differ in their Julia points. Different parameter values enhance the symmetrical pattern's beauty. It is observed that

- the parameters t, γ, μ, ν and s play a very important role in giving shape, size and color to the fractals.
- the convergence criteria derived for the fractals play a crucial role in enhancing their resolution and pixel richness.
- all the fractals developed in this paper are very novel, aesthetic, and pleasing as the function $T(z)$ and $W(z)$ incorporate a special type of sine function combined with a logarithmic component.

5. Conclusion

We derived an escape criterion for generating fractals using the proposed iterative method for the complex exponential functions $W(z) = \alpha e^{z^n} + \beta z^2 + \log \gamma^t$ and $T(z) = \sin(z^n) + \beta z^2 + \log \gamma^t$, where $n \geq 2$, $\beta \in \mathbb{C}, \gamma \in \mathbb{C}\backslash 0$, and $t \in \mathbb{R}, t \geq 1$. The visualization of Julia sets is facilitated by implementing these results in Algorithms 1 and 2. Using MATLAB software, we generated compelling non-classical variants of the Julia fractals, which were subsequently discussed and evaluated for various parameter values. We observed that these parameters significantly impact not only the shape but also the symmetry of the generated sets. We believe that the results of this research will be valuable for those interested in creating aesthetically pleasing graphics and designer printing patterns. Additionally, the textile sector can benefit from these findings for designing and printing purposes.

Acknowledgement

The authors would like to express their gratitude to the anonymous referees and editor for their valuable suggestions and helpful comments which led to significant improvement of the original manuscript of this paper.

REFERENCES

1. S. Antal, A. Tomar, D.J. Parjapati, and M. Sajid, *Fractals as Julia sets of complex sine function via fixed point iterations*, Fractal Fract., vol. 5, pp. 1–17, 2021.
2. Ashish, M. Rani, and R. Chugh, *Julia sets and mandelbrot sets in Noor orbit*, Appl. Math. Comput., vol. 228, pp. 615—631, 2014.
3. S. Cho, A. Shahid, W. Nazeer, and S. Kang, *Fixed point results for fractal generation in Noor orbit and s-convexity*, SpringerPlus, vol. 5, pp. 18-–43, 2016.
4. K. Gdawiec, W. Kotarski, and A. Lisowska, *On the Robust Newton's method with the Mann iteration and the artistic patterns from its dynamics*, Nonlinear Dynam., vol. 104, no. 1, pp. 297–331, 2021.
5. L. Jolaoso, and S. Khan, *Some escape time results for general complex polynomials and biomorphs generation by a new iteration process*, Mathematics, vol. 8, no. 12, pp. 2172, 2020.

6. L. Jolaoso, S. Khan, and K. Aremu, *Dynamics of RK iteration and basic family of iterations for polynomiography*, Mathematics, vol. 10, no. 18, pp. 3324, 2022.
7. G. Julia, *Memoire sur l'iteration des fonctions rationnelles*, Pures Appl., vol. 8, pp. 47–245, 1918.
8. S. Kumari, K. Gdawiec, A. Nandal, M. Postolache, and R. Chugh, *A novel approach to generate Mandelbrot sets, Julia sets and biomorphs via viscosity approximation method*, Chaos solitons fractals, vol. 163, pp. 112–140, 2022.
9. S. Kumari, M. Kumari, and R. Chugh, *Dynamics of superior fractals via Jungck-SP orbit with s-convexity*, An. Univ. Craiova Math. Comput. Sci. Ser., vol. 46, pp. 344–365, 2019.
10. Y. C. Kwun, M. Tanveer, W. Nazeer, M. Abas, and S. M. Kang, *Fractal Generation in Modified Jungck-S Orbit*, IEEE Access, vol. 235, pp. 35060-35071, 2019.
11. Y. C. Kwun, M. Tanveer, W. Nazeer, K. Gdawiec, and S. M. Kang, *Mandelbrot and Julia sets via Jungck-CR iteration with s-convexity*, IEEE Access, vol. 7, pp. 12167-12176, 2019.
12. P. Mainge, *The viscosity approximation process for quasi-nonexpansive mappings in Hilbert spaces*, Comput. Math. Appl., vol. 59, no. 1, pp. 74-79, 2010.
13. P. Muthukumar, and P. Balasubramaniam, *Feedback synchronization of the fractional order reverse butterfly-shaped chaotic system and its application to digital cryptography*, Nonlinear Dyn., vol. 74, no. 1, pp. 1169-1181, 2013.
14. K. Nakamura, *Iterated inversion system: An algorithm for efficiently visualizing Kleinian groups and extending the possibilities of fractal art*, J. Math. Arts, vol. 15, pp. 106-136, 2021.
15. M. Pinheiro, *s-convexity, foundations for analysis*, Differ. Geom. Dyn. Syst., vol. 10, pp. 257-262, 2008.
16. W. Phuengrattana, and S. Suantai, *On the rate of convergence of Mann, Ishikawa, Noor and SP-iterations for continuous functions on an arbitrary interval*, J. Comput. Appl. Math., vol. 235, no. 9, pp. 3006-3014, 2011.
17. M. Rani, and R. Agarwa, *Effect of stochastic noise on superior Julia sets*, J. Math. Im. Vis., vol. 36, no. 1, pp. 63-77, 2010.
18. A. A. Shahid, W. Nazeer, and K. Gdawiec, *The Picard-Mann iteration with s-convexity in the generation of Mandelbrot and Julia sets*, Monatsh. Math., vol. 195, pp. 565–584, 2021.
19. M. Tanveer, I. Ahmed, A. Raza, S. Nawaz, and Y.P. Lv, *New escape conditions with general complex polynomial for fractals via new fixed point iteration*, AIMS Mathematics, vol. 6, no. 6, pp. 5563–5580, 2021.
20. M. Tanveer, W. Nazeer, and K. Gdawiec, *New escape criteria for complex fractals generation in Jungck-CR orbit*, Indian J. Pure Appl. Math., vol. 51, pp. 1285–1303, 2020.
21. M. Tanveer, W. Nazeer and K. Gdawiec, *On the Mandelbrot set of $z^p + \log c^t$ via the Mann and Picard-Mann iterations*, Math. Comput. Simul., vol. 209, pp.184–204, 2023.
22. A. Tassaddiq, *General escape criteria for the generation of fractals in extended Jungck-Noor orbit*, Math. Comput. Simulation, vol. 196, pp. 1–14, 2022.
23. A. Tassaddiq , M. Tanveer, M. Azhar , M. Arshad and F. Lakhani, *Escape Criteria for Generating Fractals of Complex Functions Using DK-Iterative Scheme*, Fractal Fract., vol. 7, no. 1, pp. 76, 2023.
24. A. Tassaddiq , M. Tanveer, K. Israr , M. Arshad, K. Shehzad and R. Srivastava, *Multicorn sets of $\bar{z}^k + c^m$ via S-Iteration with h-Convexity*, Fractal Fract., vol. 7, no. 6, pp. 486, 2023.